Investigation of the flow structure in a cyclonic configuration for MILD Combustion processes

G. Sorrentino [1,*], P. Sabia [2], M. de Joannon [2], A. Cavaliere [1], R. Ragucci [2]

[1] DICMAPI - Università Federico II, Naples, Italy
[2] Istituto di Ricerche sulla Combustione - C.N.R., Naples, Italy
*corresponding author: g.sorrentino@unina.it

Abstract
Cyclonic flows could represent a very effective system in realizing mixing processes in very short time while allowing for a reasonable long residence time for the development of combustion reactions. This is particularly of interest in the case of high inlet temperature and diluted conditions, typical of MILD Combustion, where the fast mixing process is a need, chemical kinetics and fluid-dynamical characteristic times are comparable and the residence time play a central role in the achievement of satisfying reaction progress.
For these reasons a test chamber was built in order to perform an experimental characterization in isothermal conditions of flow fields, cyclone varying key operational parameters, such as Reynolds number of the inlet jet.
Experimental measurements were carried out in a glass windowed chamber in order to achieve a full optical access of the device and to make maintenance and cleaning operations simple.
Flow visualizations and global PIV measurements are necessary to characterize the flow field in the cyclonic flow to obtain an experimental quantification of the tangential velocity profiles into the chamber. Different inlet Reynolds number values were investigated.
A set of 3000 snapshot images were recorded for each case analyzed, then, an average image of the flow field was obtained and finally the velocity vectors.
Such measurements are significant since a characterization of cyclonic flow in terms of vortex type (forced, combined or free vortex) can be obtained.
It is possible to highlight that the flow structure appears complex and three zones can be identified for the cyclonic flow structure.

Keywords: Cyclonic flow, PIV, MILD Combustion

1 Introduction

MILD combustion [1, 2] also called FLameless OXidation (FLOX®) or High Temperature Air Combustion (HiTAC) [3, 4] is a combustion regime characterized by fuel oxidation in an atmosphere with relatively low oxygen concentration and high inlet temperatures featuring a process with a distributed reaction zone, relatively uniform temperatures within the combustion chamber, no visible flame, low noise, negligible soot formation and very low NOx and CO emissions [5, 6]. In MILD combustion, the inlet temperature of reactants is higher than the auto-ignition temperature of the mixture and, at the same time, the maximum temperature increase due to oxidation reactions remains lower than the mixture auto-ignition temperature [1, 7, 8] because of high dilution levels.
Existing industrial MILD Combustion systems usually reach the autoignition conditions by recirculating efficiently the product gases into the incoming fresh reactants [9, 10]. The exhausted gas recirculation serves two purposes: (i) to raise the reactant temperature (heat recovery) and (ii) to reduce the oxygen concentration (dilution).
To realize an efficient MILD Combustion process the establishment of an effective mixing process between the recycled gases with the fresh reactant jets can play a very important role. This in turn produces locally high turbulent mixing rates to avert the insurgence of oxidation reactions before reaching diluted conditions [11]. Thus the entrainment of products with either fuel or air and the mixing between fresh reactants remain essential processes. Another key point for MILD systems is the achievement of relatively long residence time within the combustion chamber because dilution levels imply longer kinetic characteristic times with respect to traditional systems [12, 13]. In summary the entity of recycled heat and mass, the efficiency of mixing and relatively long residence times are the key factors in the establishment of MILD combustion regimes.
The recirculation of hot reactive species into the fresh stream can be achieved through proper design of the

combustor flowfield. Flow entrainment can be obtained with different flow arrangements. It can be achieved through internal or external recirculation; however, internal recirculation is favorable for many applications. One common practice used to create entrainment and stabilize combustion can involve the use of cyclone type configuration. Cyclone combustion chambers have been reported in many forms [14]. The key factors associated with such arrangement can be summarized as follows.

(1) Longer residence time inside the combustor.
(2) Recirculation zones and turbulence generated internally by shear between differing fluid.
(3) Large toroidal recirculation zone with high level of turbulence generated for center exit configuration.

In these arrangements, the recirculation of hot active species is achieved through two key features. The first is the main jet entrainment, and the second is the recirculated gases due to the geometry of the combustor itself.
Cylindrical colorless distributed combustion incorporating tangential air injection has been investigated with emphasis on ultra-low pollutants emission and distributed reaction to explore the environmental advantages of such flows [15].
In this paper, the non-reacting flowfield of a cyclonic configuration is examined with focus on entrainment and recirculation generation in order to achieve flameless distributed combustion and enhance thermal and environmental performance of the combustor with ultra-low emissions. Non-reacting flowfield helps in understanding the flow characteristics inside the combustor along with the turbulence generated and the mixing characteristics.
In this context, a novel geometrical configuration of combustion chamber is proposed here, with the aim to realize a very fast mixing between primary and recirculated flow. The cyclonic flow pattern inside the chamber provides for large residence times and enhanced mixing between the reactants. Mixing between inlet jets and environment is analyzed and in particular the velocity field is experimentally studied through PIV analysis. The effects of the inlet jet Reynolds number on the cyclone structure and mixing process are reported.

2 Experimental facility and diagnostic

In order to study the non-reacting flowfield of a cyclonic combustion chamber, a test chamber was built in order to perform an experimental characterization under isothermal conditions, jets behavior and assessment of cyclone structure into the chamber varying key operational parameters, such as Re_{jet}. Particle Image Velocimetry (PIV) and 2D-Laser light scattering techniques were adopted to achieve these purposes. Experimental measurements were carried out in a glass windowed chamber, designed to operate at atmospheric pressure and environmental temperature conditions in order to achieve a full optical access of the device and to make maintenance and cleaning operations simple. The apparatus consists of a square section (0.2x0.2 m), in order to minimize any reflections of the laser light sheet, a height (h) of 0.05 m, inlet jets diameter (d_{jet}) of 0.008 m and a section exit placed on the top side, with a diameter (d_{out}) of 0.25 m. A sketch of the chamber illuminated by a thin laser light sheet are reported in Fig. 1. In addition to the test chamber, the experimental system is constituted by an optical detection apparatus, gas supply lines and a tracer insemination system for the flow visualization. In particular, the supply lines were made in such a way that the flow entering the test chamber was controlled and fully developed varying the inlet operating conditions. A fixed bed apparatus was used for the dispersion of the tracer particles in the gas stream.

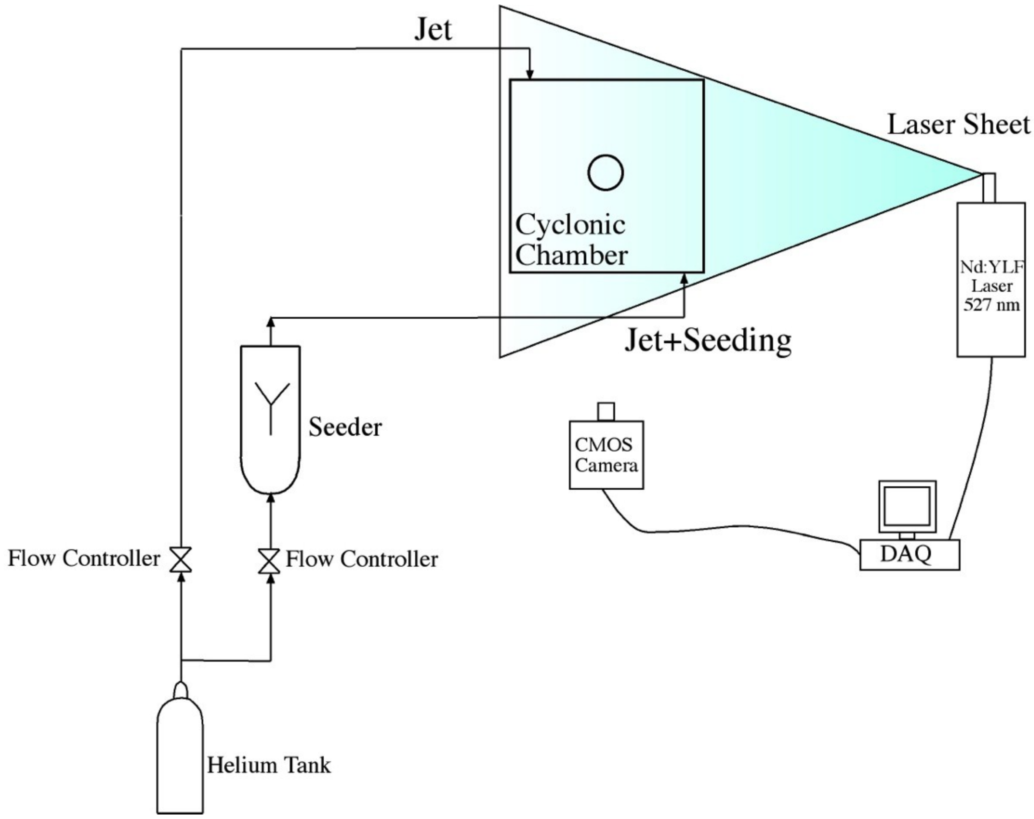

Fig. 1 A schematic diagram of the PIV setup and the test chamber

The optical characterization of the chamber is performed by recording the pattern of the light elastically scattered when a laser sheet illuminates the tracer. A Nd:YLF pulsed laser was tuned on the second harmonic wavelength (λ = 527 nm) and its beam was shaped by a set of cylindrical lenses to a sheet of constant thickness. It was varied in height by the extension of the objective field. Patterns of elastic scattered light was detected by a CMOS camera with a variable-focus telescope. Since each pulse is in a different frame, there is no directional ambiguity for the velocity vectors.
A shadow-graphic scheme has been adopted to collect images of the jets, with a proper system of lens. The pulsed laser frequency is 1000 Hz, the digital camera acquire 8-bit 1280 x 1024 pixel frames at 1000 Hz, and a BNC delay generator has been used for time base generation and synchronization. For each test condition a set of 3000 frames has been collected.
The diagnostic apparatus mainly consists of three units:
1) Laser LDY Nd:YLF double head, (λ=527 nm), maximal frequency of 10 kHz and output Energy (at 1kHz and at 527nm per laser head per pulse) of 15 mJ.
2) Camera NanoSense MkIII. Maximal resolution 1280x1024 pixels. Maximal frame rate= 2 kHz
3) A BNC 575 delay generator that manage the timebase generation and synchronization between the devices.
The laser beam is formed into a thin sheet by means of a plano-convex cylindrical lens that has a focal length of 500 mm. This is used to focus the beam near the center of the field of view of the camera. The larger Rayleigh range obtained from long focal length lenses permits also to have thicker sheets (in fact the final sheet thickness is 300 μm). In the other direction, the use of a cylindrical telescope formed from a plano-convex lens of focal length f_2=-25 mm and a larger plano-convex lens of focal length f_3=200 mm.
The reason for using two plano-convex lenses, where the convex sides are directed toward the collimated beam, is that this configuration minimizes the aberrations for a telescope formed from simple spherical lenses. The cylindrical lenses expand the laser beam only in one direction, by a factor of f_3 / f_2. In this way is possible to obtain a laser sheet of about 10 cm starting from an initial laser spot of 12 mm.
The particle density in the working fluid is set to give an average of 12 particle images in each 16 x 16 pixel interrogation window. Images for PIV were acquired at a rate of 1 kHz and the digitized images are cross-correlated using a recursive rectangular grid algorithm, which uses 32 x 32 pixel and then 16 x 16 pixel

interrogation windows to find the mean pixel displacement. A Gaussian peak fit is used to determine the location of the cross-correlation peak to sub-pixel accuracy. Post-processing comprises a standard deviation filter to remove spurious vectors, followed by an interpolation to fill any empty locations and a Gaussian smoothing. Flow visualizations and PIV measurements have been conducted under various conditions, which differ for the inlet velocity of the jets.

3 Experimental Results

Flow visualizations and PIV measurements were conducted on the global field of view 200x200 mm for obtaining information on the flow-field developed into the chamber.
All the acquisitions were carried out on the middle plane of the apparatus.
Experimental campaign was conducted varying Reynolds number of jets, based on the inlet jet diameter. The operative working conditions analyses are reported in Table 1.
Maximum capacity of the seeding generation system limits the scope of investigation to values of the Re_{jet} equal to 2000. Seeding tracer was feed in only one of the two inlet jets. Helium at 300 K was used as working fluid in order to reproduce high-temperature conditions (i.e. similar properties of CO_2 at 1000 K).

Case	***Inlet Velocity (m/s)***	***Re_{jet}***
A	*15*	*1000*
B	*22*	*1500*
C	*30*	*2000*

Table 1. Operative conditions

Global field of view measurements are necessary to characterize the fluid-dynamic field motion into the cyclonic chamber and obtain an experimental quantification of tangential velocity that provides an indication of cyclonic flow structure. Furthermore, data collected in this experimental campaign are considerably significant for comparing numerical results and testing several turbulence closure models for confined vortex flow applications.
Three different cases were investigated for the conditions reported in Table 1. In particular a value of 1000 was considered as the first value of Re_{jet} to analyze, since experimental investigations showed that such a value is critical to establish a well/defined vortex flow field into the chamber.
A set of 3000 snapshot images were recorded for each case analyzed, then, an average image of the flow field was obtained and finally the velocity vectors.
Fig. 2 shows instantaneous flow visualizations for the global field obtained with the 2D Laser Light Scattering technique, for the three different cases.
Different jet behavior can be identified, varying either the inlet jet Reynolds number or the number of jets, in terms of jet width and local structures.
The images reported in the figure are only examples and are useful to give an impression of the great variety of structures, which can be established in 3D flows.
The patterns show several vortical structures that can be identified together with the subsequent decay. In Fig. 2, it is possible to observe the first region of the jet characterized by a short laminar zone followed by very weak undulation, which quickly generates a discrete vortex. The second region constitutes a zone of evolution of successive vortices moving downstream within the mixing layer and growing in size to end finally in a chaotic zone.
Furthermore, it is worthwhile to note that the optical diagnostic apparatus is able to follow the evolution of the small-scale structures in the aforementioned range of Reynolds number.
It is worthwhile to note that the jet core length increases with the inlet Reynolds number of the jet and that its boundaries are influenced by the recirculation pattern.

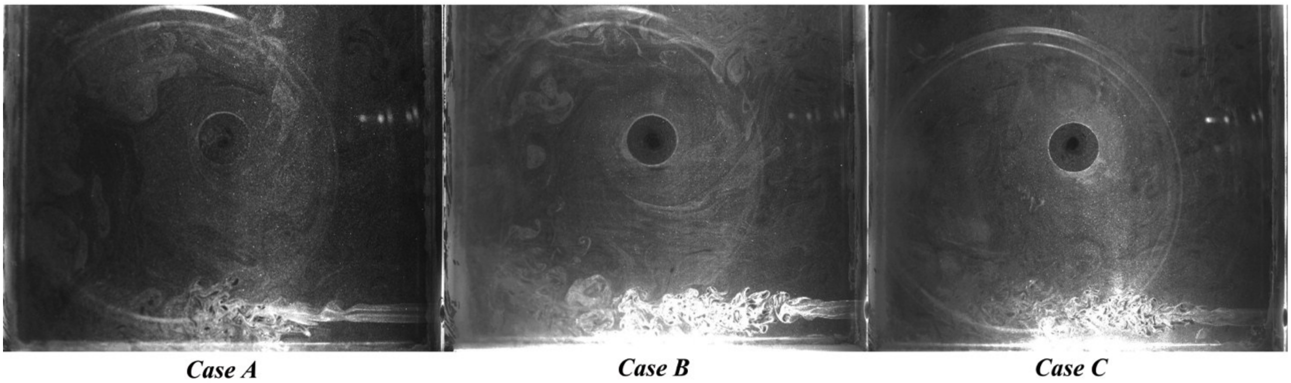

Fig. 2 Instantaneous 2D Laser Light Scattering patterns of the seeded jet

For each case PIV algorithm permits to obtain the instantaneous velocity vector. Images for PIV were acquired at a rate of 1 kHz and the digitized images are cross-correlated using a recursive rectangular grid algorithm, which uses 16 x 16 pixel interrogation windows to find the mean pixel displacement. A Gaussian peak fit is used to determine the location of the cross-correlation peak to sub-pixel accuracy. Post-processing comprises a standard deviation filter to remove spurious vectors, followed by an interpolation to fill any empty locations and a Gaussian smoothing. A post-processing analysis was performed on 3000 images for all the case analyzed. Fig. 3 shows the mean velocity vectors colored by velocity magnitude obtained by post-processing analysis.
As it is known in the literature [16], concerning the near flow field, the decay of the centerline jet velocity and jet half-width velocity are indicators, respectively, the level of fluid quantity incorporated by the jet and jet spreading.
In particular, the decay of the centerline velocity results dependent on inlet jet Reynolds number value.
It is important to highlight that jets analyzed interact with a wall. The presence of a wall causes that the maximum of jet velocity is not longer located at the jet centerline, instead it moves towards the wall. For the case analyzed such a variation is related to the interaction between the recirculated flow and jet and to the presence of wall.

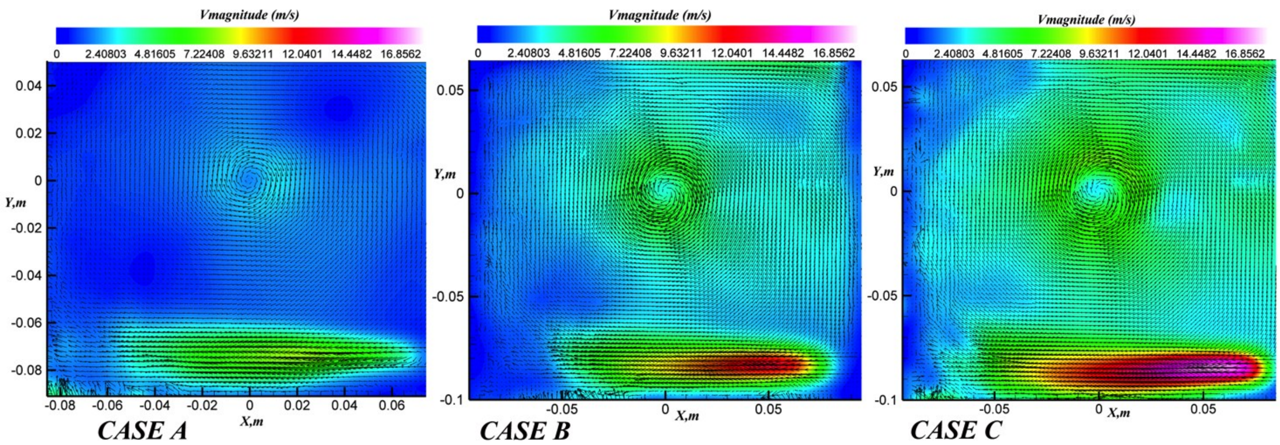

Fig. 3 Velocity vectors colored by velocity magnitude for the three cases

The experimental campaign showed that jet behavior significantly depends on inlet Reynolds number. Data collected highlighted that jets cross-interacting to form a cyclonic vortex structure show different characteristic behavior respect to a free jet in terms of velocity decay, jet width and fluid-dynamic structure.
Such a configuration demonstrates high recirculation level throughout the combustor, critical to achieve distributed combustion conditions.
The flow-field is also characterized by the presence of a high velocity region at the outer boundary with another high velocity region near the center. This behavior is almost consistent with reported velocity

behavior in cyclone combustor [17] and [18]. A detailed description of the flow pattern in a cyclone is given in the literature [14, 19], where two flows rotating coaxially and carrying the main mass of gas were described. These two flows are the wall flow and the center flow, and they are separated by a zone occupied by the rising turbulent vorticity branching from those two flows.
The characteristic profiles of tangential velocities in the chamber volume, which were measured in the midsection along the line at Y=0, are reported in Fig. 4 for the different cases.
The tangential velocity in the chamber has a typical maximum and three flow regions: the region in the center of the chamber, the region of potential rotation on the periphery of the chamber and a wall region.

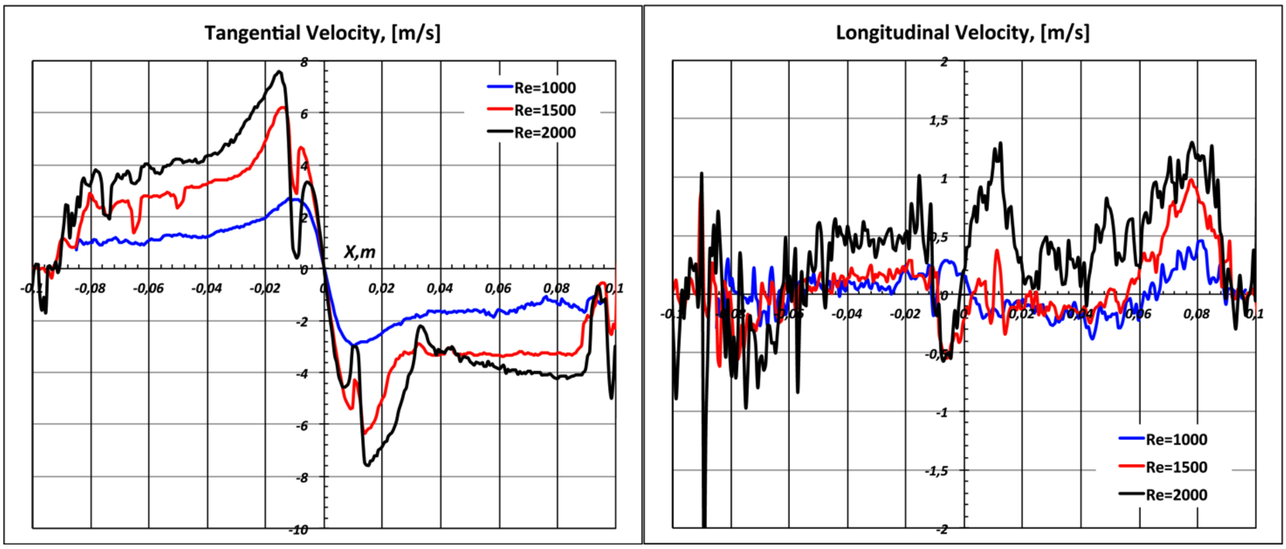

Fig. 4 Distribution of tangential and longitudinal velocities along X in the midsection for Y=0.

A somewhat larger scatter in values is observed for the dimensionless longitudinal velocity, which is due to its small magnitude and the measurement error (Fig. 4). The maximum scatter in values of the longitudinal velocity is noted near the chamber axis and is linked with the minimum value of the total velocity in this zone and with pressure pulsations.
The tangential velocity maximum increases with the inlet Reynolds number, and its position coincides approximately with the radius of the chamber outlet only for the Case A (Re=1000).
The absolute value of tangential velocity increases with the radius not monotonically for the Case B and C where a relative minimum was observed about at X=0.015 m. Such behaviour was not observed for the lower Reynolds case.
In the peripheral region of the chamber, the tangential velocity maintains almost constant values by increasing the distance from the center of the cyclone. Finally the tangential velocity approaches zero close to the wall region.

4 Conclusions

Application of MILD Combustion concept requires careful examination on the role of mixing process between fresh air-fuel mixtures with the recirculated hot products, to prepare lean and ultra-lean mixtures. In this study, a novel combustion chamber configuration, based on a cyclonic flow, was tested, in order to achieve a fast mixing between inlet and recirculated fluid inside the chamber. Non-reacting velocity measurements data are presented for the three cases with emphasis on velocity distribution. The flow-field exhibited high recirculation ratio, which enhance distributed combustion. High recirculation ratio is critical for distributed combustion as the entrainment of hot product gases is essential to form reactive and diluted oxidizer when combined with fresh air stream. The flow field was investigated by varying the inlet jet Reynolds number and the tangential velocity patterns have given an overall description of the cyclone structure.
The high velocity region near the center exhibits a non-monotone trend with the cyclone radius.
In the peripheral region of the chamber, the tangential velocity maintains almost constant values by

increasing the distance from the center of the cyclone and it approaches zero close to the wall region.
The maximum tangential velocity values and their positions result to be functions of the inlet Reynolds number of the jets.

References

[1] Cavaliere, A., de Joannon, M.: Mild combustion, *Prog. Energy Combust. Sci.* 30 (2004) 329-366.

[2] Li, P., Mi, J., Dally, B. B., Wang, F., Wang, L., Liu, Z., Chen S., Zheng, C.: Progress and recent trend in MILD combustion. *Science China Technological Sciences*, (2011), 54(2), 255-269.

[3] Wunning, J.A., Wunning, J.G. : Flameless oxidation to reduce thermal NO-formation. *Prog. Energy Combust. Sci*., 23 (1) (1997), pp. 81–94 4.

[4] Tsuji, H., Gupta, A. K., Hasegawa, T., Katsuki, M., Kishimoto, K., Morita, M. (2002). High temperature air combustion: from energy conservation to pollution reduction. CRC press.

[5] de Joannon, M., Sorrentino, G., Cavaliere, A. : MILD combustion in diffusion-controlled regimes of hot diluted fuel. *Comb. Flame*, (2012), 159(5), 1832-1839.

[6] Duwig, C., Li, B., Li, Z. S., Aldén, M. : High resolution imaging of flameless and distributed turbulent combustion. *Comb. Flame*, (2012), 159(1), 306-316.

[7] Wang, F., Mi, J., & Li, P. : Combustion Regimes of a Jet Diffusion Flame in Hot Co-flow. *Energy & Fuels*, (2013), 27(6), 3488-3498.

[8] Sabia, P., de Joannon, M., Picarelli, A., Ragucci, R. : Methane auto-ignition delay times and oxidation regimes in MILD combustion at atmospheric pressure. *Comb. Flame*, (2013), 160(1), 47-55.

[9] Abtahizadeh, E., van Oijen, J., de Goey, P.: Numerical study of mild combustion with entrainment of burned gas into oxidizer and/or fuel streams. *Comb. Flame*, (2012), 159(6), 2155-2165.

[10] Rafidi, N., Blasiak, W. : Heat transfer characteristics of HiTAC heating furnace using regenerative burners. *Appl. Therm. Eng*., 26 (2006), pp. 2027–2034

[11] Khalil A.E.E., Gupta A.K. : Distributed Swirl Combustion for Gas Turbine Application. *Applied Energy*, (2011), 88: 4898-4907.

[12] Sabia, P., de Joannon, M., Lavadera, M. L., Giudicianni, P., Ragucci, R. : Autoignition delay times of propane mixtures under MILD conditions at atmospheric pressure. *Comb. Flame*, (2014), 161 (2014) 3022-3030.

[13] Sabia, P., Lavadera, M.L., Giudicianni, P., Sorrentino, G., Ragucci, R., de Joannon, M. : CO2 and H2O effect on propane auto-ignition delay times under mild combustion operative conditions. *Comb. Flame*, (2014), 162, (3), 533–543.

[14] A.K. Gupta, D.G. Lilley, N. Syred. Swirl flows. Abacus Press, Tunbridge Wells, England, UK (1984).

[15] A.E.E. Khalil, A.K. Gupta. Swirling distributed combustion for clean energy conversion in gas turbine applications. *J Appl Energy*, 88 (2011), pp. 3685–3693

[16] Iyogun, C. O., Birouk, M. (2009). Effect of sudden expansion on entrainment and spreading rates of a jet issuing from asymmetric nozzles. *Flow, turbulence and combustion*, *82*(3), 287-315.

[17] E.D. Baluev, Y.V. Troyankin. The effect of the design parameters on the aerodynamics of cyclone chambers. *Thermal Eng*, 14 (2) (1967), pp. 67–71

[18] B.P. Ustimenko, M.A. Bukhman. Turbulent flow structure in a cyclone chamber. *Thermal Eng*, 15 (2) (1968), pp. 64–67

[19] Pitsukha, E. A., Teplitskii, Y. S., Borodulya, V. A., Volchkov, E. P., Dvornikov, N. A., & Lukashov, V. V. (2012). Investigation of the structure of swirling flows in a cyclone chamber under various conditions of gas inlet and outlet. *Journal of Engineering Physics and Thermophysics*, *85*(2), 324-338.